Numerical Predictions of Turbulence-Cascade Interaction Noise Using CAA with a Stochastic Model

V. Clair, C. Polacsek, T. Le Garrec, Marc Jacob

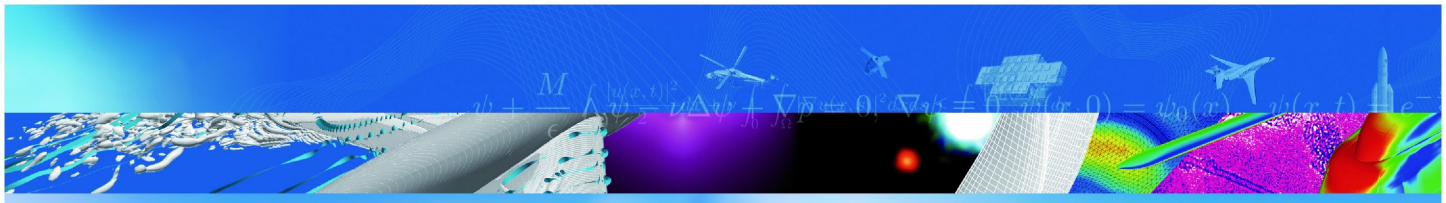

T I R É À P A R T

Numerical Predictions of Turbulence-Cascade Interaction Noise Using CAA with a Stochastic Model.

V. Clair, C. Polacsek, T. Le Garrec,
M.C. Jacob *

20th AIAA/CEAS Aeroacoustics Conference
ATLANTA, USA
16 juin-20 avril 2014

TP 2014-472

ONERA
THE FRENCH AEROSPACE LAB

retour sur innovation

Numerical Predictions of Turbulence-Cascade Interaction Noise Using CAA with a Stochastic Model.

Prévisions numériques du bruit d'interaction turbulence-cascade à partir d'un calcul CAA et d'un modèle stochastique.

par

V. Clair, C. Polacsek, T. Le Garrec, M.C. Jacob *

* Ecole Centrale de Lyon

Résumé traduit :

L'interaction des sillages turbulents avec les aubes du redresseur sont considérées comme une source de bruit à large bande contribuant fortement à l'émission sonore des moteurs d'avion en phase d'approche. Ce papier présente une méthode CAA hybride vient à simuler la réponse aéroacoustique d'une cascade annulaire impactée par une turbulence homogène isotrope prescrite. La méthode repose sur un code de calcul Euler en temporel couplé à un modèle de turbulence synthétique implanté dans le code à l'aide d'une condition aux limites adéquate proposée par Tam. Les fluctuations de pression sur la surface des aubes fournies par la CAA servent de données d'entrée à une formulation de FWH afin d'estimer le bruit rayonné. La méthode est d'abord validée sur le cas-test académique d'une rafale harmonique en interaction avec une cascade annulaire de plaques planes. Les simulations sont ensuite appliquées à des configurations d'interaction turbulence-cascade, en écoulement uniforme et en écoulement tournant, et les estimations de puissance sonore dans le conduit aval sont comparées aux solutions semi-analytiques et numériques existantes, ainsi qu'aux mesures disponibles.

NB : Ce Tiré à part fait référence au Document d'Accompagnement de Publication DSNA14048

Numerical predictions of turbulence-cascade interaction noise using CAA with a stochastic model

V. Clair[1], C. Polacsek[2], T. Le Garrec[3]
Office National d'Etudes et Recherches Aérospatiales (ONERA), 92320 Châtillon, France

M. C. Jacob[4]
Université Claude Bernard Lyon I, Laboratoire de Mécanique des Fluides et d'Acoustique, CNRS–UMR 5509 , 69622 Villeurbanne Cedex, France

Turbulent flow interactions with the outlet guide vanes are known to be mainly contributing to broadband noise emission of aeroengines at approach conditions. This paper presents a 3D CAA hybrid method aiming at simulating the aeroacoustic response of an annular cascade impacted by a prescribed homogeneous isotropic turbulent flow. It is based on a time-domain Euler solver coupled to a synthetic turbulence model implemented in the code by means of a suited inflow boundary condition proposed by Tam. The fluctuating pressure over the airfoil surface provided by CAA is used as an input to a FWH integral to calculate the radiated sound field. The method is first validated against an academic CAA benchmark in the case of a harmonic gust interacting with an annular flat plate cascade. Then, simulations are applied to turbulence-cascade interactions for annular configurations, in uniform and swirling mean flows, and numerical results in terms of sound power spectra in the outlet duct are compared to semi-analytical and numerical solutions, and to an available experiment.

Nomenclature

B	=	blade number
L	=	span
M_x, M_θ	=	axial, azimuthal mean flow Mach number
T_u	=	turbulence intensity
U_0, U_x	=	uniform, axial mean flow velocity
V	=	vane number
c	=	chord
f	=	frequency
k	=	wave number
p, p_∞	=	static pressure, undisturbed static pressure
u'	=	velocity disturbance
(x,r,θ)	=	cylindrical coordinates in the annular duct
Δk, Δf	=	wave number and frequency spacing
χ	=	stagger angle
$\phi\left(k_x,k_r\right)$	=	2-wavenumbers turbulent energy spectrum
Λ	=	integral length scale
φ	=	random phase
ρ, ρ_∞	=	density, undisturbed density
ω	=	angular frequency
(ξ,η,r)	=	local coordinates attached to the vane

[1] Research Fellow, Institute of Sound and Vibration Research, V.J.Clair@soton.ac.uk.
[2] Research Engineer, CFD and Aeroacoustics Department, cyril.polacsek@onera.fr.
[3] Research Engineer, CFD and Aeroacoustics Department, thomas.le_garrec@onera.fr.
[4] Assistant Professor, Université Claude Bernard and Polytech Lyon LMFA, marc.jacob@ec-lyon.fr.

I. Introduction

TURBULENT wakes generated by turbofan blades and interacting with the outlet guide vanes are known to be mainly contributing to broadband noise emission of aeroengines at approach conditions. Analytical approaches, such as Amiet[1] isolated airfoil or Hanson[2] cascade models can be adopted to estimate the noise generated by turbulent flows impacting thin airfoils, but they are limited by the flat-plate assumptions. Despite some recent attempts[3-5], reliable rotor-stator turbulent interaction sources are still out of reach of common CFD solvers based on LES or DES approaches. These simulations are generally restricted to a radial strip and to a single vane channel by enforcing periodicity conditions, and it should be more considered for capturing the 3D turbulent wake behind an isolated rotor blade as investigated in Ref. 6. Recently, the Lattice-Boltzmann Method (LBM) have been firstly applied to turbomachinery noise problems with an impressive direct acoustic simulation performed by EXA[7] on the Nasa Glenn Advanced Noise Control Fan model, including the full rotor-stator stage and the wind tunnel walls. The LBM technique appears a quite promising way to face present limitations in terms of current CPU capabilities.

Another approach based on a CAA/Euler hybrid methodology coupled to a synthetic turbulence inflow can also be considered, as investigated by recent studies[8-10], and is the object of the present paper. Here, we suggest to numerically assess the aerodynamic response of annular grids impacted by a prescribed turbulent velocity field, instead of using airfoil or cascade flat plate response models adopted in the semi-analytical prediction tools. The turbulent (blade) wake generation, devoted to CFD, is discarded in the present study.

The method is described in the first part of the paper, focusing on the way of modeling and injecting a synthetic turbulent flow (in terms of solenoidal velocity disturbances) in a CAA Euler code developed at Onera[11,12], respectively using a prescribed isotropic homogeneous TKE (Turbulence Kinetic Energy) spectrum expanded into spatial Fourier modes, and a suited BC (Boundary Condition) proposed by Tam[13].

In the second part, the numerical simulations are validated against an academic benchmark related to a 3D annular cascade impacted by a swirling harmonic gust in a uniform axial mean flow proposed by Namba & Schulten[14]. The CAA results are compared to the semi-analytical solutions addressed by Namba[15] and Schulten[16]. For this test case, the acoustic response of the cascade (in-duct sound field) is directly assessed by the CAA.

Then the method is applied to the simulation of turbulence-cascade interaction noise on two selected configurations:

- A turbulence-annular cascade interaction in a uniform axial mean flow, related to a laboratory experiment performed in the anechoic open jet wind tunnel of Ecole Centrale de Lyon[17] ;

- A turbulence-annular cascade interaction in a swirling mean flow, related to a benchmark proposed by Atassi & Vinogradov[18], with a reference solution issued from the frequency-domain linearized Euler code developed by Atassi[19].

For these more complex cases, the CAA domain is limited to a single vane channel, and sound radiation in the outlet duct is obtained by means of a FWH integral (restricted to the loading noise term and using pressure fluctuations along vane surface as input data), and assuming a fully uniform flow in the propagation (even for the swirling mean flow case). The present numerical predictions of in-duct Power Spectrum Density (PSD) in the outlet duct (downstream of the cascade) are compared to available measurements and analytical solutions too, issued from Amiet theory extended to ducted fans[20,21] and advanced 3D lifting surface calculations[22].

II. Hybrid method based on stochastic model coupled to CAA

The simulations are performed using the ONERA code *sAbrinA.v0*[11,12] solving the full Euler equations in the time domain with a perturbation form that consists in a splitting of the conservative variables into a mean flow and a disturbance field. Aiming at performing rotor-stator interaction problems through CAA calculations, efficient numerical BC (asymptotic solutions of the linearized Euler equations) derived by Tam[13] have been implemented in the code[10] to allow velocity perturbations to be imposed at the inflow boundary. Although Tam's boundary conditions are initially written in 2D polar coordinates, a more suited form extended to spherical coordinates[23] is used for ducted cascade calculations. As done in Ref. [23], a sponge zone (over-filtering) is applied too at the exit of the CAA domain in order to permit both hydrodynamic and acoustic outgoing waves to leave the domain without creating numerical reflections. The proposed stochastic model is almost identical to Kraichnan's theory[24]. As proposed by Kraichnan and also adopted in Ref [25], it is based on a Fourier-mode decomposition of the incoming turbulent wake modeled as an HIT (homogeneous isotropic turbulence) energy spectrum, but restricted here to the upwash velocity component (normal to the airfoil assimilated to a flat plate) by analogy with Amiet's theory. Moreover, in order to limit the size of the CAA domain and CPU cost, and following the approach of Casper and Farassat[26], the synthetic turbulence is described by a 2-wave numbers spectrum (the 3D HIT spectrum is integrated over the azimuthal wave numbers), with a spatial distribution over streamwise and spanwise directions. Thus,

neglecting the azimuthal wave number dependency of the TKE spectrum, the 2-wave numbers spectrum approach suggested by Clair[10] for simulating turbulence-airfoil problem is re-considered here for present annular cascade configurations. These restrictions are discussed in the applications presented in section IV. Hence, the incoming gusts (tangential component u'_θ only), in the case of a purely axial mean flow and annular cascade with zero stagger angle, can be written as:

$$u'_\theta(x,r,t) = 2\sum_{i=1}^{N}\sum_{j=-M}^{M}\sqrt{\phi_{u_\theta u_\theta}\left(k_{x,i},k_{r,j}\right)\Delta k_x \Delta k_r}\cos\left(k_{x,i}x + k_{r,j}r - \omega_i t + \varphi_{i,j}\right) \tag{1}$$

In Eq. (1), the mode amplitude is fitted by a Von-Karman or Liepmann energy spectrum $\phi\left(k_x,k_r\right)$, defined by two parameters: the turbulence intensity (T_u) and the integral length scale (Λ). Considering a frozen turbulence, the turbulent structures are assumed to be convected through the undisturbed upstream flow (mean velocity U_x), so that the angular frequency ω is related to the streamwise (axial) wave number k_x (aligned to the vane chord) by:

$k_x = \omega/U_x$. $\varphi_{i,j}$ is a random phase chosen between 0 and 2π associated to each mode (i,j). The synthetic turbulent field so obtained is solenoidal (divergence free), which prevents it from creating any spurious sound sources.

Although sound propagation might be directly assessed by CAA as done in section III related to harmonic gust-cascade interactions, it is practically obtained by a coupling to a FWH formulation (loading noise term) using a Green's function valid for annular ducts and uniform axial mean flow[20,21].

III. Validations on academic NASA benchmark

Firstly, our numerical method has been validated against 3rd CAA benchmark cases proposed by NASA[10], devoted to the simulation of a swirling harmonic gust interacting with an annular cascade (V = 24 flat plates with chord c = 1 m) in an axial uniform mean flow (M = 0.5). The inflow velocity disturbances using cylindrical coordinates (x,r,θ) are defined as:

$$\begin{cases} u'_r(r,\theta,x,t) = 0 \\ u'_\theta(r,\theta,x,t) = A\cos\left(k_x x + m_g\theta + k_r\left(r - r_h\right) - \omega t\right) \\ u'_x(r,\theta,x,t) = -\dfrac{m_g}{rk_x}u'_\theta(r,\theta,x,t) \end{cases} \tag{2}$$

In Eq. (2), A is the gust amplitude, m_g is the gust azimuthal order, and the radial wave number k_r is equal to $\dfrac{2\pi q}{r_t - r_h}$, where q is an integer, r_h and r_t are the inner and outer radius, respectively.

The following parameters are considered: r_h = 24/4p (m), $r_t = 2r_h$ (m), $f_0 = \omega/2\pi$ = 177.5 (Hz), A = 0.1 U_0 (m/s), and m_g = 16.

Applying the well-known Tyler & Sofrin condition ($m = nB - kV$, with $B = m_g$) and a periodicity condition in the azimuthal direction, the CAA domain can be restricted to a $2\pi/8$ angular sector covering 3 vane channels. A 3D view of the mesh is shown in Fig. 1. The grid is extending from -4 chords (upstream) to 12 chords in the axial direction, and a very fine grid spacing of about 1/500 chord is imposed in the vicinity of the leading and trailing edges. Respectively 370, 46, and 181 cells are used in the axial, radial, and azimuthal directions, which totalizes 3.2 M points. Since Tam's BC are not actually able to avoid reflections of outgoing spinning acoustic modes, a local stretching (coefficient equal to 1.03) associated to a sponge zone is applied at the exit (downstream) of the grid domain. A converged solution requires about 30 hours of CPU time over 120 processors.

Typical snapshots of the computed disturbance fields (tangential velocity and pressure) for the cases q = 0 and q = 3, repeated over a full revolution, are presented in Fig. 2. The expected dominant acoustic cut-on mode m = -8 is clearly recovered, and the damping zone mentioned above allows making the sound waves exit the domain without creating noticeable numerical reflections.

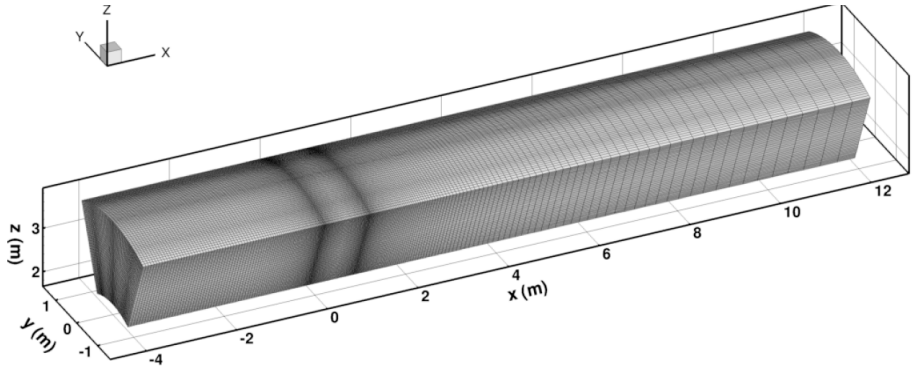

Figure 1. 3D annular grid (3 vane channels) used for the CAA benchmark

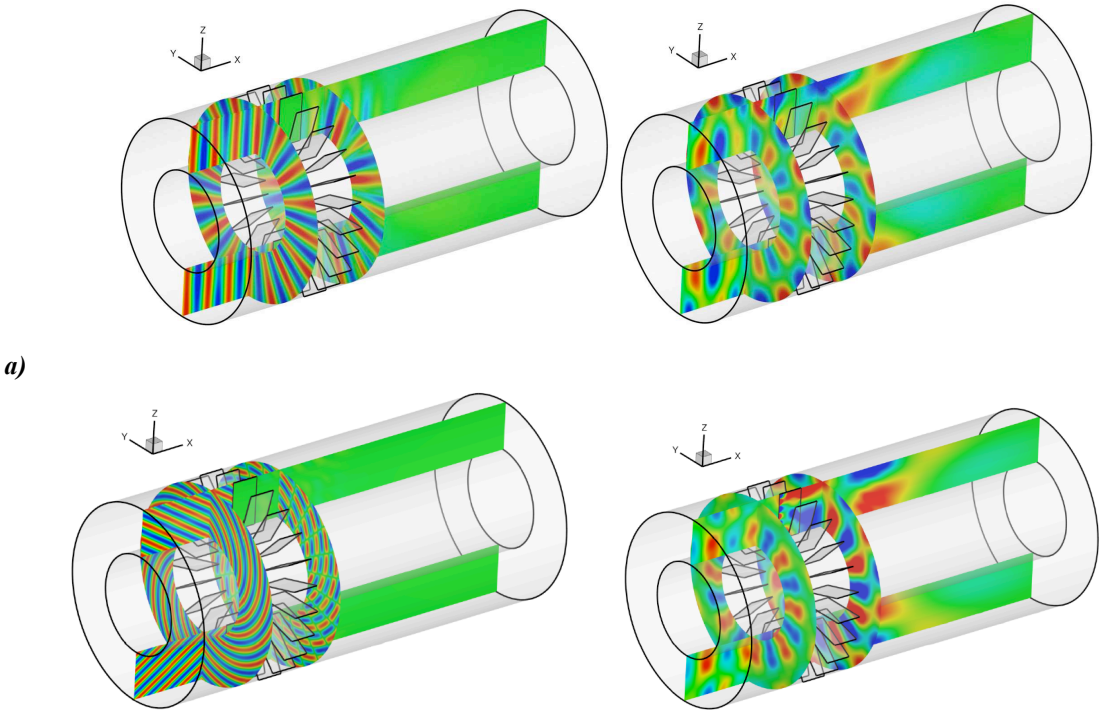

a)

b)

Figure 2. Snapshots of tangential velocity (m/s, left) and pressure (Pa, right) disturbances duplicated over a full revolution for the cases $q = 0$ (a) and $q = 3$ (b)

Radial distributions over the vane surface of the harmonic wall pressure component ($f = f_0$) provided by CAA are compared to available semi-analytical solutions of Schulten[14] in Fig. 3, for case $q = 3$. The agreement is excellent, with only slight differences close to the trailing edge ($x = 0.9\ c$).

Finally, the modal amplitude and phase of the acoustic pressure obtained from a Fourier-Bessel transformation over a selected cross-section at $x = 2c$ (2 chords downstream the cascade), are compared in Figure 4 to the solutions of Namba & Schulten[14] for $q = 0$, 1, 2, 3 and cut-on modes (-8,1), (-8,2), (-8,3). Again, a fairly good agreement is observed for all cases.

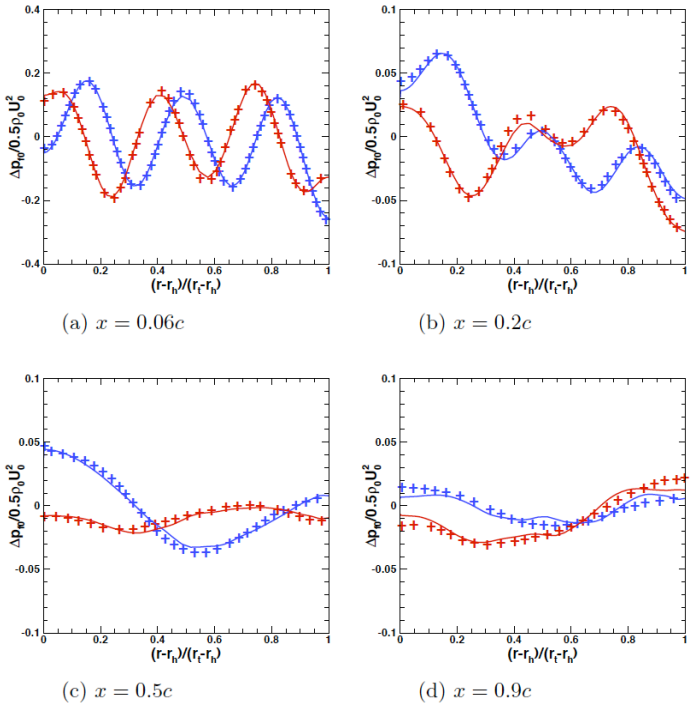

Figure 3. Harmonic normalized pressure over the vane surface for q = 3:
CAA results (—) compared to Schulten results (+) ; Real part (blue) and imaginary part (red)

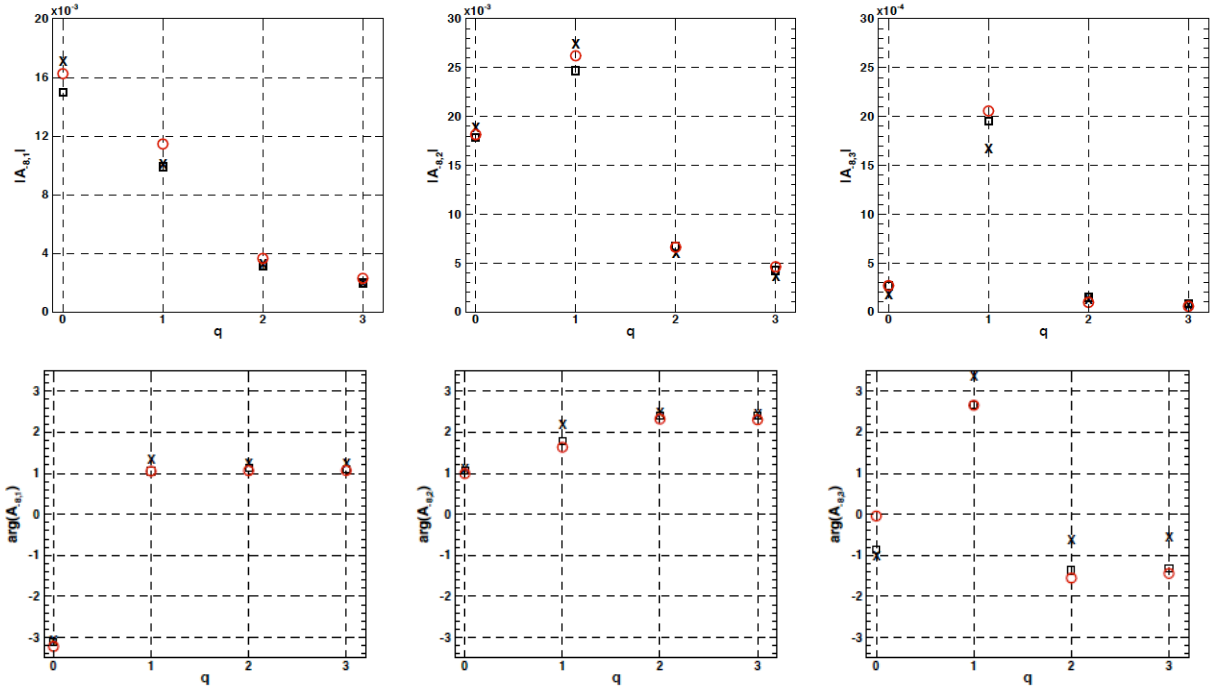

Figure 4. Modal amplitude (top) and phase (bottom) issued from Fourier-Bessel transform at x = 2c:
m = -8 (m = 1 to 3) and q = 0,1,2,3 ; CAA results (O) compared to Schulten (□) and Namba (x)

IV. Applications to turbulence-annular cascade configurations

The previous single harmonic gust simulations have been extended to broadband noise by considering a synthetic turbulent inflow obtained from an HIT spectrum. Two application cases are discussed below, considering purely axial and swirling mean flows, respectively.

A. Turbulence-annular cascade interaction in a uniform axial mean flow

A first validation case is devoted to a turbulence-cascade interaction using a turbulence grid in a purely axial mean flow, related to an experiment proposed by ECL[17]. A picture of the anechoic open-jet wind tunnel with an outlet view of the model and a sketch of the test rig are shown in Fig. 5.

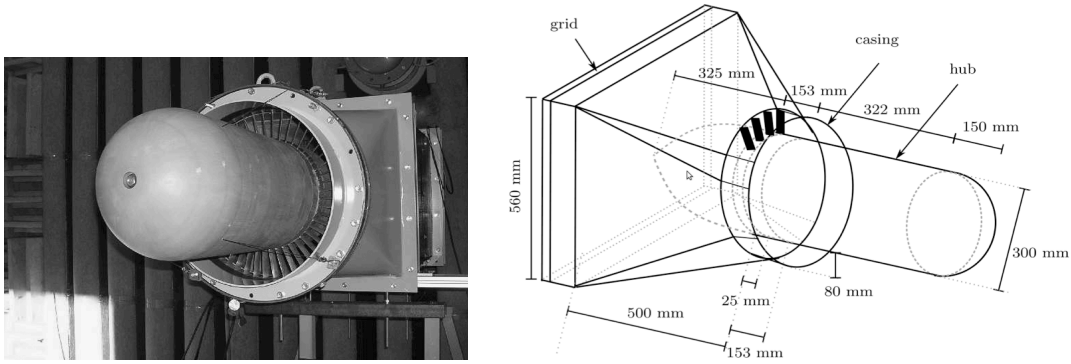

Figure 5. ECL open-jet anechoic wind tunnel experiment (left) and sketch of the rig (right)

Two selected turbulence grids (T1,T2) with respective averaged turbulence intensity $T_1 \approx 3.5$ % and $T_2 \approx 6$%, and two cascades (C1,C2) with respective vane numbers $V_1 = 49$ and $V_2 = 98$ were investigated. The flat plate vanes have an $L = 80$ mm span, a c = 25 mm chord and a $\chi = 16.7°$ stagger angle (with a zero degree angle of attack). The inner and outer radii of the annular duct are respectively is $r_h = 150$ mm and $r_t = 230$ mm, and the axial velocity is $U_0 = 80$ m/s. T1 and T2 grids gave an estimated integral length scale Λ almost equal to 20 mm when fitting the hotwire measurements to the Liepmann HIT model.

The 2-wave number Liepmann spectrum expressed in cylindrical coordinates in the *x*-duct frame writes:

$$\phi_{u_\theta u_\theta}(k_x,k_r) = \frac{3\overline{u}_\theta'^2\Lambda^2}{4\pi}\frac{k_x^2\Lambda^2 + k_r^2\Lambda^2}{\left(1+k_x^2\Lambda^2+k_r^2\Lambda^2\right)^{5/2}} \tag{3}$$

In Eq. (3), the turbulent upwash velocity, u_θ', is related to the turbulence intensity, T_u, as $\overline{u}_\theta'^2 = T_u^2 U_0^2$. Present CAA simulations are performed on T2-C1 case and the main parameters are summarized in the Table 1.

Table 1. Annular cascade parameters relative to ECL case T2-C1 considered in the CAA

r_h (mm)	r_t (mm)	c (mm)	V	χ (°)	U_0 (m/s)	Λ (mm)	T_u
150	230	25	49	0	80	19.9	0.06

For the sake of simplicity, the stagger angle is set to zero in the simulations because the effect on turbulence-airfoil noise is expected to be quite small. Indeed, calculations of sound power spectra in the outlet duct issued from an Amiet-based code developed by Reboul[20] (considering an isolated airfoil response model and a Green's function valid for annular ducts) and setting $\chi = 0°$ or $\chi = 16.7°$ provide almost identical results (see Fig. 6). Furthermore, as already explained in section II, the incoming turbulence can be restricted to parallel gusts ($k_r = 0$ in Eqs. (1) and (3)), as done in the Amiet theory and suggested by Reboul[20,21] for turbofans with span-to-chord ratio $L/c > 3$. It was also verified numerically by Clair[10] for turbulence-airfoil simulations. As explained in Ref. 10, this is simply achieved in the CAA by setting $\Delta k_r = \frac{2\pi}{L}$ in Eq. (1).

In order to check the reliability of our Amiet-based predictions, a comparison with solutions obtained by Posson[17] and Zhang[22] is proposed in Fig. 7, in which the experimental result is plotted too. The T1-C1 case was recently investigated by Zhang[22] who addressed a quite relevant solution based on the lifting surface method of Schulten[16], generalized to broadband noise. Zhang's result for the T1-C1 case has been extrapolated to the T1-C2

case in Fig. 7b by simply applying a frequency dependant correction factor that is equal to the ratio of corresponding Liepmann spectra. For both cases, the three predictions are reasonably close with a 3-4 dB over-estimate of Reboul's results compared to those of Zhang, that can be partly attributed to cascade effects neglected in the Amiet isolated airfoil theory, although Amiet-based predictions better fit the experiment (the low-frequency hump beyond 500 Hz visible on the spectra has to be related to an additional noise caused by installation effects[17]). The 3D lifting surface method expected to be the most rigorous one, provides rather similar results to the quasi-3D cascade model of Posson in the high frequency range, whereas the PWL spectrum of Reboul displays a lower level attenuation slope.

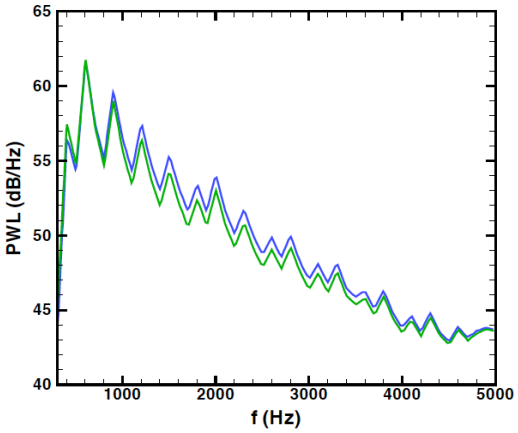

Figure 6. PWL spectra (dB/Hz) in the outlet duct provided by Amiet-based calculation on T2-C1 case and setting $\chi = 16.7°$ (green) or $\chi = 0°$ (blue)

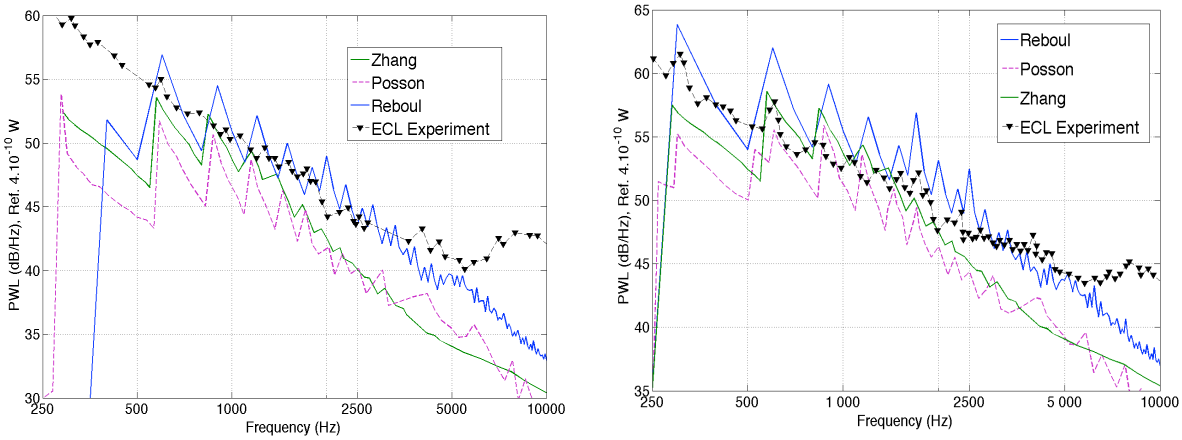

Figure 7. Comparison of PWL spectrum solutions obtained by three different calculation methods for T1-C1 (left) and T2-C1 (right) cases

The use of a simplified turbulence spectrum representation, $\phi(k_x,0)$, without azimuthal dependence, allows us to limit the CAA domain to a single vane channel by applying suitable periodicity conditions in the angular direction (and so to greatly reduce the CPU costs). Thus, the CAA domain is restricted to a $2\pi/V$ sector leading to a 3D grid of about 1.5 M cells. The CAA grid characteristics are summarized in the table 2. The synthetic turbulent inflow is injected for frequencies ranging from 300 Hz to 5000 Hz, with a frequency resolution Δf = 100 Hz. Hence, a complete period $T = 1/\Delta f$ is achieved after 85,000 time iterations, requiring 27 hours of CPU time over 64 processors.

Table 2. CAA grid characteristics

N_x	N_r	N_θ	*Axial extent (m)*	*radial extent (m)*	*Azimuthal extent (m)*
373	51	81	$-0.1 < x < 0.25$	$0.15 < r < 0.23$	$-\pi/49 < \theta < \pi/49$

Although the Amiet theory is only valid for an isolated airfoil, cascade effects should be taken into account here by the use of periodicity conditions, traducing the influence of adjacent vanes on the aerodynamic response of the airfoil. However, the restriction to planar gusts, which means setting $m_g = 0$ in Eq. (2), does not allow anymore to directly assess the acoustic response, as done with harmonic gusts in section III. Indeed, only interaction modes $m = \pm kV$ can be created, and as gust-airfoil interactions occur in-phase for all vanes, interference effects between dipole-sources of adjacent vanes lead to a quasi null radiated field. This point is illustrated in Fig. 8, showing snapshots of azimuthal velocity disturbances (fig. 8 left) and pressure disturbances (fig. 8 right) over a 3D annular slice corresponding to the CAA domain duplicated over 3 angular sectors. The planar shape of the multi-harmonic gusts is clearly highlighted as well as the dipolar source response of each vane, giving rise to a noise cancellation in the upstream and downstream directions due to destructive interference effects. Anyway, the fluctuating wall pressure over the vane surface is expected to be reliable, and the radiated sound field can be computed by means of a FWH analogy. This is practically achieved by chaining the CAA output to an in-house code solving the loading noise term of FWH formulation (with an in-duct modal Green's function) written in the frequency domain.

The RMS surface pressure over the vane is plotted in Fig. 9 showing an expected source concentration in the leading edge region. Chordwise RMS pressure profiles (normalized by $\rho_0 U_0^2$) computed by the CAA at hub (green), mid-span (red) and casing (blue) locations, are compared to Amiet's (isolated airfoil) solution in Fig. 10. A reasonable agreement can be observed, but the levels of the computed profiles are slightly below the Amiet solution: this might be attributed to cascade effects that are taken into account in the CAA.

Finally, the CAA-FWH computations (in red) in Fig. 11, are compared to analytical solutions of Zhang (green), Posson (pink) and Reboul (blue). The PWL spectrum issued from the numerical simulations clearly displays a reduction of about 3 dB compared to the Amiet-based solution of Reboul, in accordance with the wall pressure analyzes discussed in Fig. 10. The numerical prediction is very close to the 3D lifting surface solution, but it better fits the experiment at high frequencies beyond 2000 Hz for which the PWL spectrum provided by CAA is less attenuated than the predictions of Zhang and Posson.

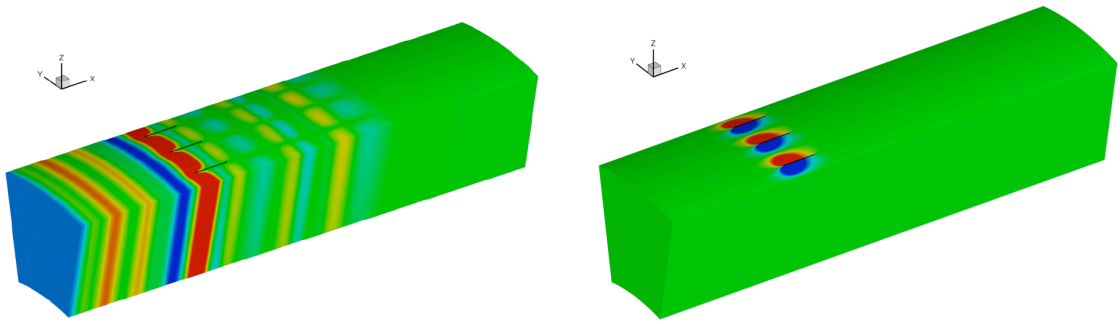

Figure 8. Snapshot of azimuthal velocity disturbances (± 2.5 m/s, left) and pressure disturbances (± 100 Pa, right) duplicated over 3 angular sectors

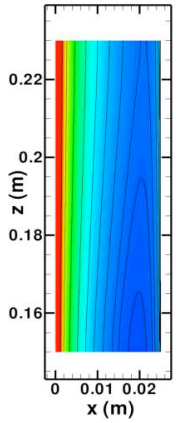

Figure 9. RMS surface pressure (Pa)

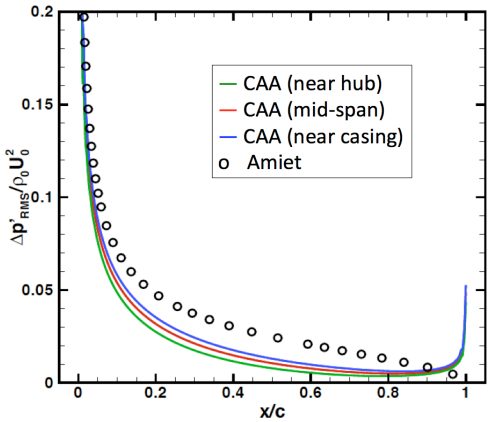

Figure 10. Chordwise RMS pressure profiles (normalized) issued from CAA and Amiet

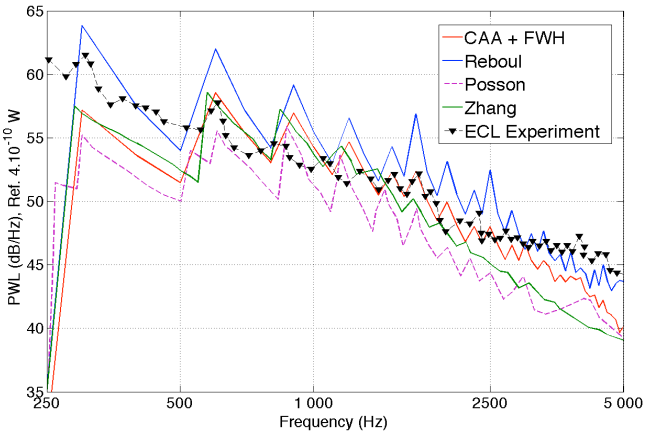

Figure 11. PWL spectra (dB/Hz) provided by calculations (CAA+FWH & analytical solutions) and compared to experiment for T2-C1 case

B. Turbulence-annular cascade interaction in a swirling mean flow

The second application case concerns a benchmark proposed by Atassi & Vinogradov[18], related to an annular grid of $V = 45$ unloaded flat plates with 160 mm chord in a swirling mean flow. The vanes are twisted with a suited stagger angle χ varying along the span and adjusted so that the angle of attack remains equal to zero (local chord aligned with the streamlines). The characteristics of the annular duct are $r_h = 0.99$ m and $r_t = 1.65$ m. The swirling mean flow is imposed by an axial and azimuthal component (the radial component being set to zero). The azimuthal Mach number is defined as (setting $\Omega = \Gamma = 0.125$):

$$M_\theta(\bar{r}) = \Omega\bar{r} + \frac{\Gamma}{\bar{r}} \tag{4}$$

Using Crocco equation and neglecting the entropy and enthalpy variations, the axial Mach number can be written as:

$$M_x(\bar{r}) = \sqrt{M_x^2(r_{moy}) - 2\left[\Omega^2\left(\bar{r}^2 - 1\right) + 2\Omega\Gamma\ln(\bar{r})\right]} \tag{5}$$

r_{moy} is set equal to 1.32 m, which corresponds to a total Mach number equal to 0.5.
Main parameters are summarized in the table 3, in which $\bar{r}$ is the radius normalized by its mid-span value.

Table 3. Swirling mean flow and stagger angle values

$r(m)$	$\bar{r}$	M_θ	M_x	$\chi\ (^o)$
0.99	0.75	0.2604	0.4681	29.1
1.32	1.00	0.2500	0.4330	30.0
1.65	1.25	0.2563	0.3949	33.0

The mean static pressure field is derived from the radial momentum equilibrium:

$$p(\bar{r}) = p_\infty\left[1 + (\gamma - 1)\left\{\left(\frac{\bar{r}^2 - 1}{2}\right)\left(\Omega^2 + \frac{\Gamma^2}{\bar{r}^2}\right) + 2\Gamma\Omega\ln(\bar{r})\right\}\right]^{\gamma/(\gamma-1)} \tag{6}$$

In Eq. (6), $\gamma = 1.4$, and $p_\infty = 101986$ Pa. The mean density field is defined as: $\rho(\bar{r}) = \rho_\infty\left(\frac{p(\bar{r})}{p_\infty}\right)^{1/\gamma}$.

The Cartesian coordinates $(x_\zeta, y_\zeta, z_\zeta)$ of a point ζ along a vane in the curvilinear frame (ξ, η, r) sketched in Fig. 12 can be expressed as:

$$\begin{cases} x_\zeta(r) = \xi\cos\left(\chi(r)\right) \\ \alpha_\zeta(r) = \dfrac{\xi\sin\left(\chi(r)\right)}{r} \\ y_\zeta(r) = -r\sin\left(\alpha_\zeta(r)\right) \\ z_\zeta(r) = r\cos\left(\alpha_\zeta(r)\right) \end{cases} \tag{7}$$

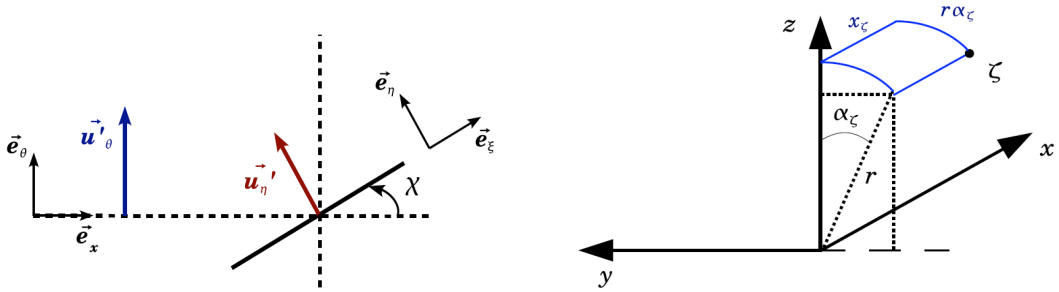

Figure 12. Local frames attached to the duct and to the vane (left) and Cartesian coordinates related to curvilinear points (right)

A 3D representation of the annular grid with colored stagger angle varying from 29° to 33° is shown in Fig. 13, and the CAA grid made of about 1.4 M points (limited to a single vane channel) is visualized in Fig. 14. The computation parameters are summarized in the table 4.

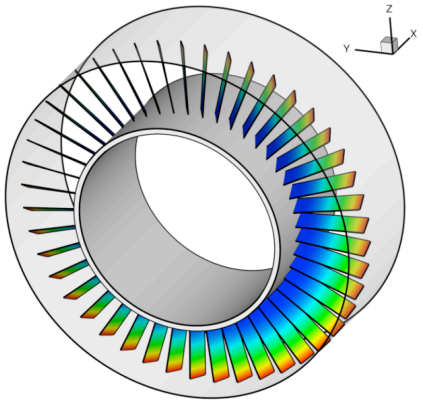

Figure 13. 3D representation (full revolution) of annular grid with colored stagger angle

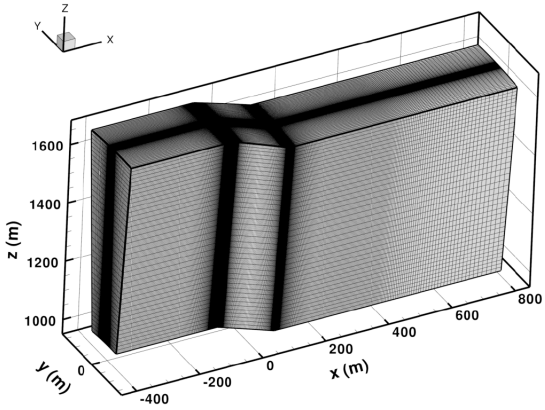

Figure 14. CAA 3D grid of single vane channel

Table 4. CAA grid characteristics

N_x	N_r	N_θ	*Axial extent (m)*	*radial extent (m)*	*Azimuthal extent (m)*
417	41	85	$-0.4 < x < 0.8$	$0.99 < r < 1.65$	$-\pi/45 < \theta < \pi/45$

Due to the fact that the vane chord is not aligned with the duct axis anymore, the synthetic turbulent inflow injected into the CAA frame with Cartesian coordinates (x,y,z) related to the duct cylindrical coordinates (x,r,θ) has to be expressed with respect to the local vane curvilinear coordinates (ξ,η,r). Thus, restricting again to the parallel gusts ($k_r = 0$) and introducing the stagger angle χ, the velocity disturbances of Eq. (1) are re-written as:

$$\begin{cases} u'_\theta(x,r,\theta,t) = 2\sum_{i=1}^{N} A_i \cos\left(k_{x,i}x - \omega_i t + \varphi_i\right) \\ A_i = \sqrt{\dfrac{\phi_{u_\eta u_\eta}\left(k_{\xi,i}x,0\right)\Delta k_\xi \Delta k_r}{\cos(\chi(r))}} = \sqrt{\dfrac{\phi_{u_\eta u_\eta}\left(k_{x,i}x\cos(\chi(r)),0\right)\Delta k_x \cos(\chi(r))\Delta k_r}{\cos(\chi(r))}} \end{cases} \quad (8)$$

The wave numbers k_x and k_ξ being linked since $k_\xi = k_x \cos\chi$ and $x_\zeta = \xi_\zeta \cos\chi$, the axial phase term $k_x x$ in Eq. (3) is actually equal to $k_\xi \xi$ at the vane wall. One should note that by projection of u'_θ, a component u'_ξ will be also added to the upwash component u'_η. However, this fluctuations are sliding along the chord and are not expected to generate any sound. The azimuthal velocity disturbances as well as the pressure dististurbances are plotted on Fig. 15

As for the previous case, the restriction to parallel gusts (k_r = 0 in Eq. (3)) in order to reduce the CPU cost is justified by the practical requirement $L/c \geq 3$. However, this simplification proposed by Amiet[1] for isolated airfoils and checked by Reboul[20,21] for ducted fans is valid for non-varying inflow conditions along the span which is no more true here. The parallel gust restriction in the CAA then might be questionable and will be discussed below.

As defined by Atassi, the turbulence is modeled using the Liepmann TKE spectrum, with constant parameters T_u = 1.8% and $\Lambda \approx$ 42 mm. Harmonic gusts are injected with a frequency spacing Δf = 100 Hz up to f_{max} = 3300 Hz. About 16,500 time iterations are required to simulate a complete period and a converged result is reached after 2 periods, requiring only 12 hours of CPU time over 64 processors.

3D snapshot views of azimuthal velocity and pressure disturbances can be visualized in Fig. 14, left and right, respectively. As explained above, the wave fronts are almost normal to the duct axis and not to the vanes. The wave front lean traduces the radial variations of the mean flow. Wall pressure distributions provided by CAA over lower and upper vane sides are plotted in Fig. 16 (right), for several spanwise positions, and compared to the Amiet solution. A rather good agreement can be observed, despite a non-symmetrical response with slightly higher levels predicted by the numerical simulations. It can be seen that the normalized RMS pressure levels are almost constant in the spanwise direction as highlighted by iso-pressure contour maps plotted in Fig. 16 (left).

The PWL spectrum in the outlet duct is then calculated by coupling the CAA output data (vane surface pressure) to the FWH solver (solid surface formulation). In Fig. 17, our CAA result (in red) is compared to Atassi's solution (in black) digitized from Ref. [18] and also to the Amiet-based prediction (in blue). Although the turbulent inflow conditions are set constant, the Amiet calculation is performed by splitting the duct into several radial strips (10 in the present case) in order to account for mean flow and stagger angle variations in the spanwise direction. A very good agreement can be observed between Atassi and Amiet-based predictions, which tends to show that the cascade effects should be negligible for this configuration. On the other hand, the present CAA solution significant differences, with lower PWL and particularly a steep attenuation slope beyond 1500 Hz. This leads to an underprediction of - 8 dB/Hz around 3000 Hz). Such differences with the Amiet result are surprising regarding to the low discrepancies observed on the RMS wall pressure distributions (in Fig. 16 right).

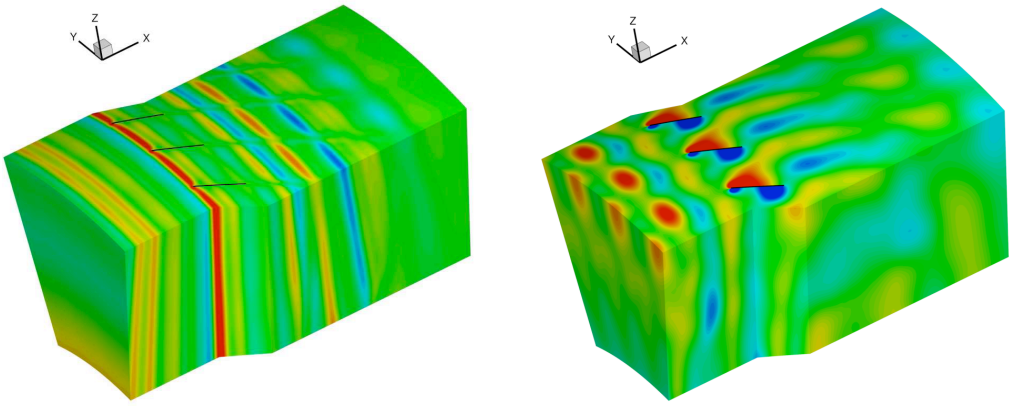

Figure 15. Snapshot of azimuthal velocity disturbances (± 2 m/s, left) and pressure disturbances (± 100 Pa, right) duplicated over 3 angular sectors

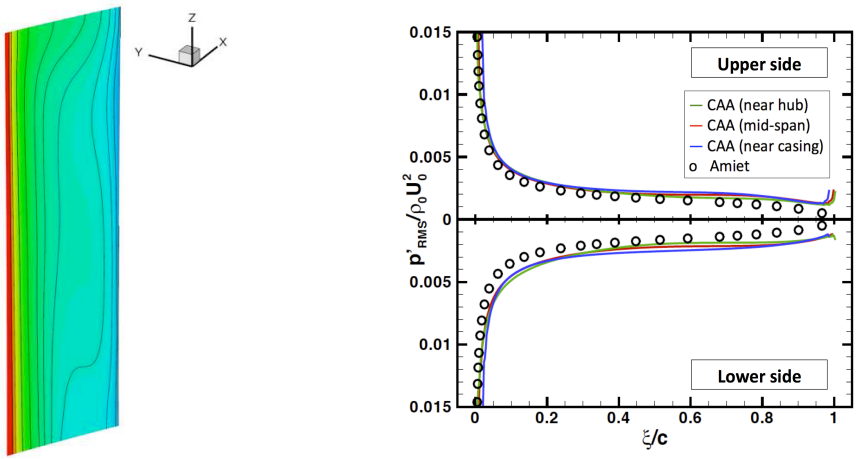

Figure 16. CAA surface RMS pressure (Pa) over lower vane side (left)
and chordwise normalized RMS pressure profiles at 3 spanwise stations compared to Amiet solution (right)

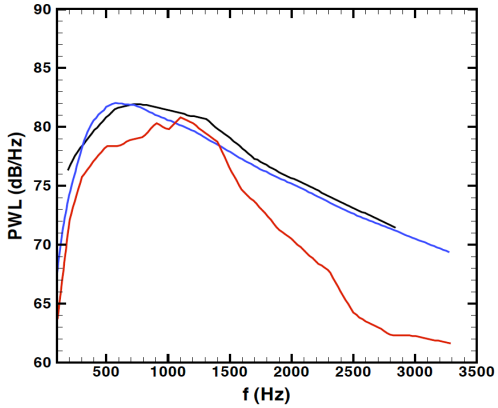

Figure 17. PWL spectra (dB/Hz) provided by CAA+FWH (red)
and compared to Atassi (black) and Amiet-based (blue) predictions

In order to better understand the reasons for this mismatch, wall pressure spectra have been analysed. A typical result is shown in Figs. 18 and 19, comparing pressure PSD level and phase at two chordwise positions with Amiet's model (Fig. 18 an 19 respectively). Near the leading edge the shape and level of the computed spectra are found to be rather close to the Amiet predictions (in dotted lines), but important oscillations seem to appear at 10% chord. Nevertheless, the mean value of the oscillating level versus frequency, for each spanwise position, is not far from Amiet's reference solution. An explanation for these discrepancies shown in Fig. 17 can been inferred from Fig. 19, where significant phase variations between radial stations at 10% chord (Fig. 19 right) can be seen in the frequency range [2000-3300 Hz]. Destructive interference effects could result from these phase shifts along the span, when integrating the wall pressure fluctuations in the FWH solver (whereas in Amiet's approach with parallel gusts, sources are expected to be all in-phase in the spanwise direction). As mentioned before, the parallel gust restriction in the CAA might not be suited to realistic configurations with mean swirling flows.

To check this point, a FWH calculation has been run again by discarding the phase information along the span (source correlation is only considered in the chordwise direction). The numerical prediction obtained by this way is plotted in Fig. 20 and compared to the previous solutions, showing an increase of the PWL up to 3 dB/Hz and leading to a better agreement with Atassi's results. This tends to confirm our interpretation and provides some limits of our present numerical method when discarding the oblique gusts.

New simulations using complete 2-wavenumbers turbulence spectrum $\phi(k_x, k_r)$ are planned, but are still requiring an optimization of the source term calculation with respect to processors loading during parallelization process in order to reduce the CPU time.

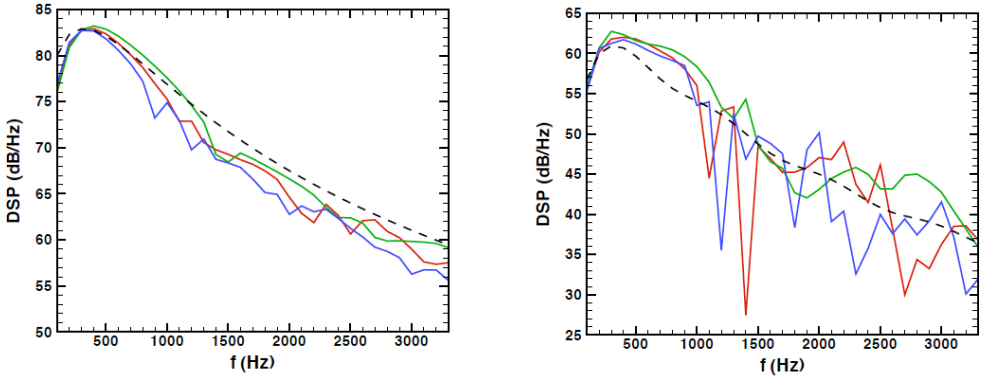

Figure 18. CAA wall pressure PSD (dB/Hz) on vane pressure side (hub/green, mid-span/red, casing/blue) compared to Amiet solution (dotted line) at $\xi/c \approx 0$ (left) and $\xi/c = 0.1c$ (right).

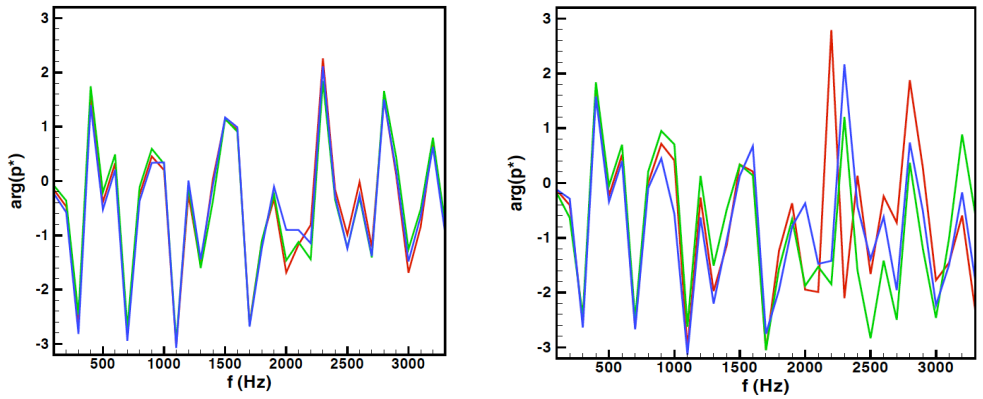

Figure 19. CAA wall pressure PSD phase (radians) on vane pressure side (hub/green, mid-span/red, casing/blue) at $\xi/c \approx 0$ (left) and $\xi/c = 0.1c$ (right).

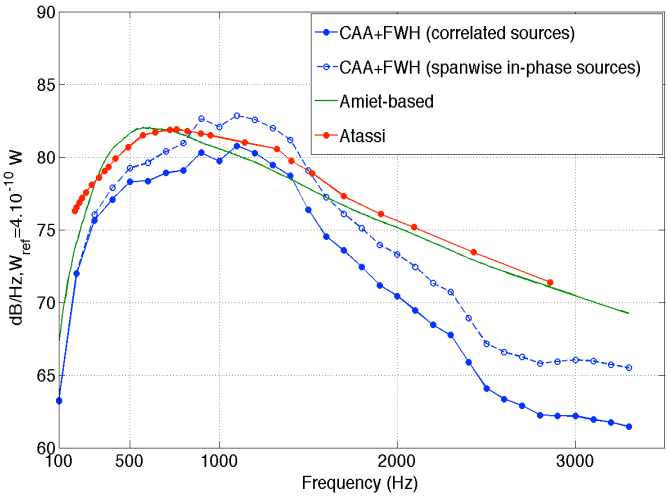

Figure 20. PWL spectra (dB/Hz) provided by CAA+FWH (blue) compared to Atassi (red) and Amiet-based (green) solutions

V. Conclusions and Future Work

A hybrid methodology based on a 3D CAA/Euler solver coupled to a stochastic model aiming at generating a synthetic turbulent inflow has been presented in this paper. Suited Tam's boundary conditions have been implemented into the code to ensure a non-reflecting injection of velocity disturbances, and have been associated to a sponge zone at the exit for outgoing acoustic/hydrodynamic modes. Simulations have been conducted on annular cascade configurations with prescribed inflow disturbances impinging the flat-plate vanes. Both uniform and swirling mean flow cases have been investigated, and the numerical predictions have been successfully compared to semi-analytical solutions and to experimental data (when available). Sound propagation simulatuions in the duct are practically achieved by chaining the CAA to a FWH solver.

The present method has been first validated against a CAA benchmark proposed by NASA, showing an excellent agreement. A 2-wave numbers (streamwise and spanwise) turbulence spectrum integrated in the azimuthal direction has been suggested in order to limit the computation domain to a single vane channel. Furthermore, by analogy with the Amiet theory, synthetic turbulence can be restricted to parallel gusts (setting spanwise the wave number equal to zero). This allows us to considerably reduce the CPU costs. Our predictions are found to be very close to reference solutions when the mean flow is purely axial. A first application to a more realistic swirling mean flow case (involving a radial evolution of the convection flow and stagger angle) seems to show that the spanwise wave number contribution has to be included into the CAA simulations in order to provide a more reliable numerical prediction.

Our computations are currently extended by including a complete 2-wavenumbers turbulent spectrum, which requires much higher CPU resources. The next issue is to apply the method to SDT configuration from NASA Glenn[27] recently proposed as a benchmark for a new workshop on "turbofan broadband noise predictions".

Acknowledgements

This work was conducted in the framework of the LabEx CeLyA ("Centre Lyonnais d'Acoustique") of Université de Lyon, operated by the French National Research Agency.

References

[1]Amiet, R. K., *Acoustic radiation from an airfoil in turbulent stream*, J. Sound and Vib., **41**(4), pp. 407-420, 1975.

[2]Hanson, D., *Broadband noise of fans. with unsteady coupling theory to account for rotor and stator reflection/transmission effects*, NASA Contractor Report 211136, 2001.

[3]Riou, J., Léwy, S. & Heib, S., *Large eddy simulation for predicting rotor-stator broadband interaction fan noise*, Inter-noise2007 Conference, 2007.

[4]Greschner, B. & Thiele, F., *Wall modeled LES simulation of rotor-stator-cascade broadband noise*, 17th AIAA/CEAS Aeroacoustics Conference, AIAA Paper 2011-2873, 2011.

[5]Laborderie, J., Moreau, S. & Berry, A., *Compressor Stage Broadband Noise Prediction using a Large-Eddy Simulation and Comparisons with a Cascade Response Model*, AIAA Paper 2013-2042, 2013.

[6]Li, Q., Peake, N., and Savill, M., *Large Eddy Simulations for Fan-OGV Broadband Noise Prediction*, AIAA Paper 2008-2843, 2008.

[7]Mann, A., Perot, F., Kim, M.-S., Casalino, D. & Fares, E., 2012, *Advanced noise control fan direct aeroacoustics predictions using a Lattice-Boltzmann method*, 18th AIAA/CEAS Aeroacoustics Conference, no AIAA-2012-2287.

[8]Dieste, M., and Gabard, G., *Synthetic Turbulence Applied to Broadband Interaction Noise*, 15th AIAA/CEAS Aeroacoustics Conference, AIAA Paper 2009-3267, 2009.

[9]Wohlbrandt, A., M., Guerin, S., Ewert, R., *Simultaneous Computation of Surface and Volume Sources for Fan Broadband Noise with the Random-Particle-Mesh Method*, 19th AIAA/CEAS Conference, AIAA Paper 2013-2119.

[10]Clair, V., Polacsek, C., Le Garrec, T., Reboul, G., Gruber, M. & Joseph, P., *Experimental and Numerical Investigation of Turbulence-Airfoil Noise Reduction Using Wavy Edges*, AIAA Journal, Vol. 51, No. 11, pp. 2695-2713, 2013.

[11]Redonnet, S., Manoha, E., and Sagaut, P., *Numerical Simulations of Propagation of Small Perturbations Interacting with Flows and Solid Bodies*, 7th AIAA/CEAS Aeroacoustics Conference, Paper 2001-0222, 2001.

[12]Redonnet, S., Desquesnes, G., Manoha, E., and Parzini, C., *Numerical study of acoustic installation effects with a computational aeroacoustics method*, AIAA Journal, **48(5)**, 2010.

[13]Tam, C. K. W., *Advances in Numerical Boundary Conditions for Computational Aeroacoustics*, Journal of Computational Acoustics, Vol. 6, No. 4, pp. 377–402, 1998.

[14]Namba, M. & Schulten, J., *Third computational aeroacoustics (CAA) workshop on benchmark problems: Category 4 — fan stator with harmonic excitation by rotor wake*, NASA Technical Memorandum, 2000-209790, pp. 73-85, 2000.

[15]Namba, M., *Three-dimensional analysis of blade force and sound generation for an annular cascade in distorted flows*, *J. Sound and Vib.*, **50**, p. 479-508, 1977.
[16]Schulten, B., *Sound generated by rotor wakes interacting with a leaned vane stator*, *AIAA Journal*, **20(10)**, p. 1352-1358, 1982.
[17]Posson, H. & Roger, M., *Experimental validation of a cascade response function for fan broadband noise predictions*, *AIAA Journal*, Vol. 49, No. 9, p. 1907-1918, 2011.
[18]Atassi, H. & Vinogradov, I., *Modeling broadband fan noise and comparison with experiments*, *13th AIAA/CEAS Aeroacoustics Conference*, AIAA Paper 2007-3691, 2007.
[19]Atassi, H., Ali, A., Atassi, O. & Vinogradov, I., *Scattering of incident disturbances by an annular cascade in a swirling flow, Journal of Fluid Mechanics*, **499**, p. 111-138, 2004.
[20]Reboul, G., Polacsek, C., Lewy, S. & Heib, S., *Ducted-fan broadband noise simulations using unsteady or averaged data*, Inter-noise2008 Conference, 2008.
[21]Reboul, G., *Modélisation du bruit à large bande de soufflante de turboréacteur* [In French], PhD, Ecole Centrale de Lyon, 2010.
[22]Zhang, W., Wang, X. & Sun, X., *A broadband noise model for turbulence/annular cascade interaction*, 19th AIAA/CEAS Aeroacoustics Conference, AIAA Paper 2013-2243, 2013.
[23]Bogey, C. & Bailly, C., *Three-dimensional non-reflective boundary conditions for acoustic simulations: far-field formulation and validation test cases*, Acta Acustica, **88**, p. 463-471, 2002.
[24]Kraichnan, R., *Diffusion by a random velocity field*, Physics of Fluids, **13(1)**, p. 22-31, 1970.
[25]Salem Said, A.-H., *Large Eddy Simulation of Shear-Free Interaction of Homogeneous Turbulence with a Flat-Plate Cascade*, PhD Thesis, Virginia Polytechnic Institute and State University, 2007.
[26]Casper, J. & Farassat, F., *Broadband noise predictions based on a new aeroacoustic formulation*, 40th Aerospace Sciences Meeting and Exhibit, AIAA Paper 2002-0802, 2002.
[27]Woodward, R.P., Hugues, C.E., Jeracki, R. J. & Miller, C. J., *Fan noise source diagnostic test — Far-field acoustic results*, 8th AIAA/CEAS Conference, AIAA Paper 2002-2427, 2002.

ONERA
THE FRENCH AEROSPACE LAB

BP 72 - 29 avenue de la Division Leclerc - 92322 CHATILLON CEDEX - Tél. : +33 1 46 73 40 40 - Fax : +33 1 46 73 41 41

www.onera.fr